



ELSEVIER

Biophysical
Chemistry

Biophysical Chemistry 81 (1999) 59–80

www.elsevier.nl/locate/bpc

Protein adsorption at the oil/water interface: characterization of adsorption kinetics by dynamic interfacial tension measurements

C.J. Beverung, C.J. Radke, H.W. Blanch*

Department of Chemical Engineering, University of California, Berkeley, CA 94720, USA

Received 4 June 1999; received in revised form 14 June 1999; accepted 14 June 1999

Abstract

The dynamics of protein adsorption at an oil/water interface are examined over time scales ranging from seconds to several hours. The pendant drop technique is used to determine the dynamic interfacial tension of several proteins at the heptane/aqueous buffer interface. The kinetics of adsorption of these proteins are interpreted from tension/log time plots, which often display three distinct regimes. (I) Diffusion and protein interfacial affinity determine the duration of an initial induction period of minimal tension reduction. A comparison of surface pressure profiles at the oil/water and air/water interface reveals the role of interfacial conformational changes in the early stages of adsorption. (II) Continued rearrangement defines the second regime, where the resulting number of interfacial contacts per protein molecule causes a steep tension decline. (III) The final regime occurs upon monolayer coverage, and is attributed to continued relaxation of the adsorbed layer and possible build-up of multilayers. Denaturation of proteins by urea in the bulk phase is shown to affect early regimes. © 1999 Elsevier Science B.V. All rights reserved.

Keywords: Protein adsorption; Interfacial tension; Liquid/liquid interfaces

* Corresponding author. Tel.: +1-510-643-7255; fax: +1-510-643-1228.
E-mail address: blanch@socrates.berkeley.edu (H.W. Blanch)

1. Introduction

As naturally occurring macromolecules, proteins and their milieu are of interest to numerous scientific disciplines. The behavior of proteins in the body is the subject of intensive medical research efforts in fields such as disease characterization, disease prevention, protein transport, and nutrition. Large-scale production while maintaining protein structure, activity, and nutritive value is the focus of the pharmaceutical and food processing industries. Knowledge of the interactions of proteins with their changing environments, especially over time, is necessary for studies in these fields.

Interfacial concentration of proteins at the oil/water interface is often the subject of research in protein-stabilized food emulsions. Dickinson [1,2] has applied the technique of specular neutron reflectivity [3] at the *n*-hexane/water interface to determine surface concentration of protein films. Results indicate surface concentration values of 2–3 mg/m² for β -casein and 1–2 mg/m² for globular proteins after adsorption from dilute bulk solutions. Surface viscosity of these adsorbed films displays opposite trends, with globular protein films maintaining two to three orders of magnitude larger viscosities than films of β -casein. This difference has been attributed to larger flexibility of the disordered β -casein molecules. A technique using radiolabeled β -casein to measure surface concentrations at the oil/water interface shows similar results, with values of \sim 3 mg/m² [4].

Knowledge of the thickness of adsorbed protein films is necessary to understand the role of proteins in emulsion and foam stability. A wide range of results has emerged for adsorption of β -casein at various interfaces. Ellipsometric techniques [5,6] have shown thicknesses as low as 5 nm at the air/water interface. Photon correlation spectroscopy indicates layers up to 15 nm thick for β -casein bound to polystyrene particles [7]. Neutron reflectivity [1] data suggest a double layer forms at fluid interfaces, with a dense inner layer immediately at the interface with a thickness of 2

nm, and a diffuse layer extending 5–7 nm into the water phase. While the results using these spectroscopic techniques slightly vary, order of magnitude comparisons with typical protein diameters (2–5 nm) indicate layers corresponding to less than 10 monolayer thicknesses. None of these methods have, as yet, been used to extensively study adsorption of globular proteins at an oil/water interface.

The formation of a viscoelastic film at the oil/water interface due to protein adsorption has been observed. Interfacial viscosities of proteins adsorbed at the oil/water interface show a distinct time dependence [8]. Low viscosities are seen (< 1 mN/m/s) for three proteins during the initial minutes of interfacial exposure. After 72 h, the values are protein-dependent, from 200 (lysozyme) to 60 (β -casein) to < 1 mN/m/s (β -casein). Transient development of large limiting film strengths for many globular proteins adsorbed at the oil/water interface has also been noted [9].

The adsorption of proteins to a fluid interface is commonly studied by determining the interfacial tension between the two phases [5,8,10–26]. As proteins adsorb to an oil/water interface, dynamic trends in the reduction of interfacial tension give an indication of the characteristic subprocesses at play in the early stages of adsorption. We determine the interfacial tension as a function of time for several different protein solutions to obtain information on the effects of structural and chemical variables on adsorption at the oil/water interface. Often, it is more convenient to express the data as a change in tension from the pure fluid value. This change is defined as the surface pressure

$$\Pi(t) = \sigma_0 - \sigma(t) \quad (1)$$

where σ_0 is the interfacial tension of the pure fluids. Thus, surface pressure increases from zero during protein adsorption, and surface pressure/ \log time plots are the mirror image of tension/ \log time plots. This notation allows for easy comparison of systems with different σ_0 .

2. Materials and methods

Dynamic interfacial tension was measured using the pendant drop technique. This method is useful for the time regimes of interest in protein adsorption from dilute solution, and is commonly used elsewhere [22,24,27–29]. Computer automation allows rapid drop image acquisition, edge detection, and fitting of the Young–Laplace equation to determine the interfacial tension. Fig. 1 is a schematic of the apparatus used here. Ovalbumin, β -casein, lysozyme, bovine serum albumin, wheat germ lipase, and *Candida rugosa* lipase were obtained from Sigma Chemical and used without further purification beyond dialysis. Recombinant glutamate dehydrogenase from the extreme thermophile *Pyrococcus furiosus* was obtained from Professor Douglas Clark (UC Berkeley). *n*-Heptane (Fisher 99% spectrophotometric grade) was filtered through a column of roasted silica beads and contacted with water for 24 h to obtain a saturated oil phase. Aqueous solutions

were made using distilled, deionized water from a Millipore filtration unit (resistivity = 15 M Ω /cm). Monobasic and dibasic sodium phosphate buffer salts (Fisher, certified ACS grade) were used in ratios corresponding to the desired pH and ionic strength. All experiments were conducted at room temperature ($22 \pm 1^\circ\text{C}$). The interfacial tension of filtered heptane/Millipore water shows a slow reduction from 51.0 to 49.5 mN/m over a period of 24 h.

3. Results

3.1. Ovalbumin

Ovalbumin is a globular protein in the serine protease inhibitor (serpin) superfamily, purified from chicken egg white. This protein is well characterized structurally and, thus, is an excellent candidate for testing the effects of a number of different chemical variables on its adsorption dy-

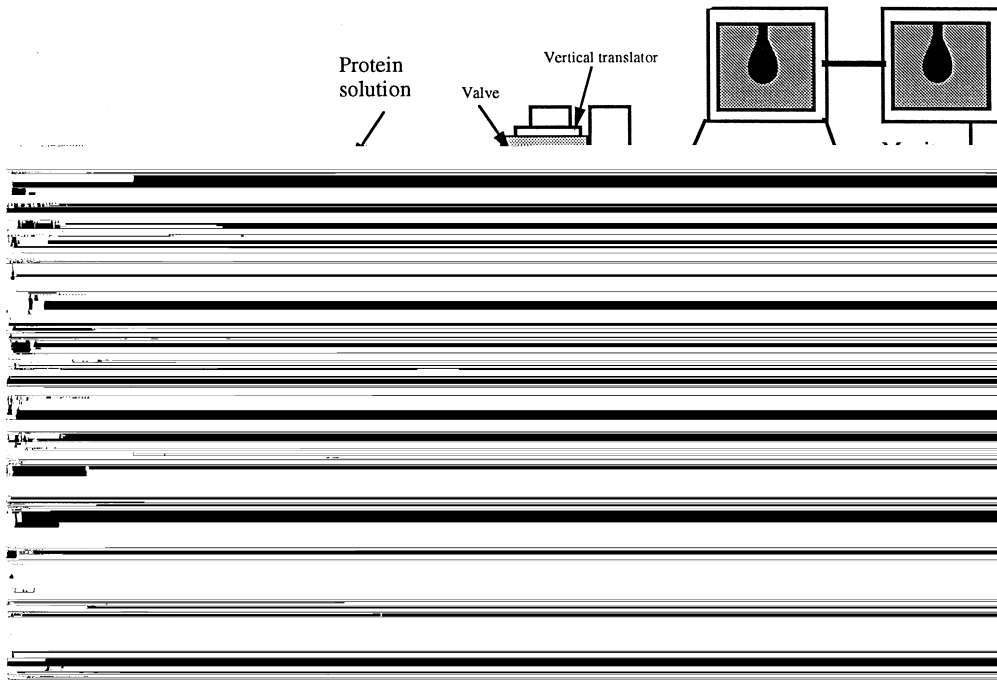


Fig. 1. Pendant drop apparatus.

namics. Ovalbumin has a molecular weight of 42 kDa, one disulfide bond, and four free sulfhydryl groups. The isoelectric point is 4.6 and, thus, the protein is negatively charged at neutral pH. The crystal structure is known [30], and shows that the molecule is almost completely involved in secondary structure, with nine α -helices and three β -sheets. Ovalbumin is ellipsoidal, with approximate molecular dimensions of $70 \times 45 \times 50 \text{ \AA}$.

Fig. 2 shows the concentration dependence of ovalbumin interfacial tension dynamics at the heptane/buffer interface. The buffer solution is 100 mM ionic strength sodium phosphate at pH 7.1. At low concentration, there is an initial lag time where the interfacial tension remains near the water/heptane value of 51 mN/m. This can be described as a diffusion-limited regime, where the interface is lacking a sufficient quantity of protein to noticeably change the tension. As the interface becomes saturated, the rate of tension decrease is high as indicated by the curve in the 20–90-s regime. At surface pressures of ~ 10 mN/m, the dilute ovalbumin solution adsorption dynamics exhibit an abrupt change to a less rapid rate of decline. This final regime, which appears as a constant slope on the tension–log time plot, may be attributed to a slow conformational rearrangement of the interfacial film. The apparent logarithmic-kinetic-dependence may also be affected by protein aggregation and the construction of a rigid network. After 24 h, a decrease in tension is still apparent, suggesting that this globular protein needs a significant amount of time to seek an equilibrium interfacial conformation. At higher concentrations (50, 100 $\mu\text{g}/\text{ml}$), the initial lag time is not seen, and the systems immediately seek the third regime of decreasing interfacial tension kinetics.

To test the hypothesis that protein denaturation at the oil/water interface is vital to strong film formation and occurs over a long time frame, tests were performed using urea-denatured ovalbumin. In the highly denatured state, the internal non-covalent interactions maintaining native structure are disrupted, mobilizing the protein and allowing it to behave as a random coil capable of achieving many conformational isomers. By

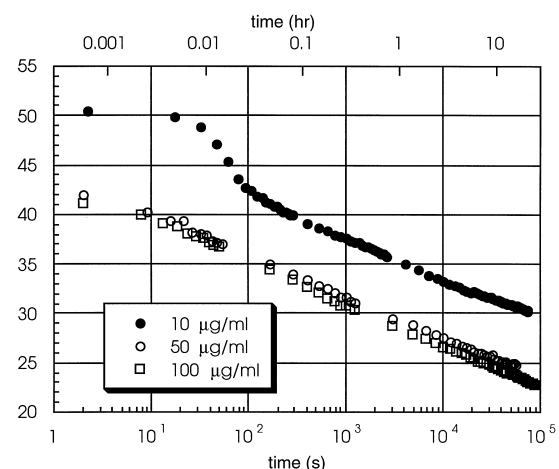


Fig. 2. Dynamic interfacial tension of ovalbumin at the heptane/aqueous buffer interface, pH = 7.1, 100 mM sodium phosphate buffer.

relaxing the native structure of the protein before it diffuses to the interface, the time dependence of interfacial denaturation can be probed. Different levels of bulk denaturation are achieved by exposure to various concentrations of urea. For ovalbumin, it has been shown that denaturation begins at urea concentrations of 6 M and becomes fully denatured at 9 M [31]. Since protein-free urea solutions showed negligible surface activity at the oil/water interface, dynamic interfacial tension of ovalbumin/urea solutions allow investigation of denaturation effects. Fig. 3 shows the dynamic surface pressure of dilute ovalbumin solutions at 0, 6, and 9 M urea concentrations. Initially, it can be seen that for all systems, a characteristic diffusional lag time is present. An initial tension reduction is seen to be most rapid in the urea-free system, where the surface pressure reaches 8 mN/m at $t \sim 100$ s. At this point, the profile changes slope, and is logarithmic at a more gradual slope thereafter. This is in contrast to the concentrated urea solutions, which exhibit much slower kinetics of adsorption. However, over extended periods of time, higher urea concentrations promote more rapid rates of increase of surface pressure and larger final values.

These trends suggest that denaturation plays a key role in the kinetics of protein adsorption.

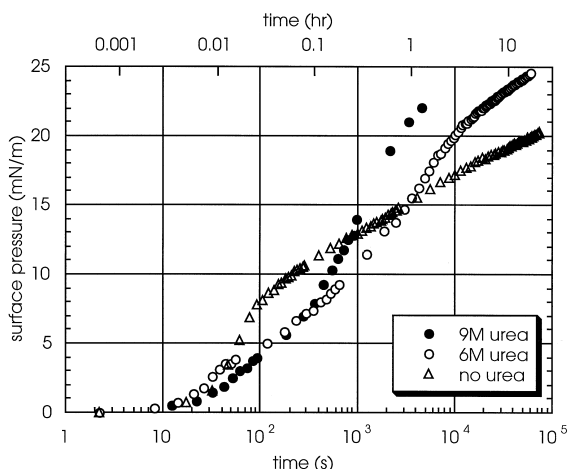


Fig. 3. Dynamic surface pressure of urea-denatured ovalbumin solutions adsorbing at the heptane/buffer interface. Protein concentration $C_b = 10 \mu\text{g/ml}$, pH = 7.5, 100 mM sodium phosphate buffer.

One may expect that a large degree of denaturation helps the exposed hydrophobic groups of the protein seek and arrange themselves in the oil environment, shortening the time to achieve certain values of surface pressure. This does not appear to be the case at early times, where the urea-free system exhibits a faster increase in surface pressure. Non-denatured proteins adsorb strongly and quickly proceed into slowly decreasing tension regimes, where interfacial conformational changes become important in determining tension reduction. Since concentrated aqueous urea is a favorable solvent for both hydrophobic and hydrophilic entities, the driving force for adsorption of hydrophobic groups to the oil phase is reduced when the protein is in a urea solution. This weaker attraction also slows the rearrangement process of hydrophobic side chains attempting to reach the oil phase. These groups eventually do encounter the interface, and at longer times the protein/urea solutions achieve greater pressures than the urea-free system. The difference between the 6 and 9 M urea solutions suggests that denaturation plays a more important role in the second time regime. Once adsorbed, a greater number of side chains may be able to orient themselves in the interface as higher urea

concentrations provide increased flexibility of the molecules. Proteins in 6 M urea take longer to complete their interfacial rearrangements, leading to a later surface pressure increase in the second time regime. These effects may also encourage gel formation. As with urea-free adsorption, ovalbumin in concentrated urea solutions exhibits slow increases in surface pressure at very long times and the formation of visible interfacial films or gels that collapse when internal volume is withdrawn.

In this work, protein charge effects were also examined using ovalbumin. We have shown that protein surface charge plays a major role in adsorption of charged synthetic amino acid copolymers [32]. Charge effects are dependent on the dielectric nature of the solvent, and hence are often screened in high ionic strength buffer solutions. At pH 7.1, ovalbumin has a net charge of -12 that is localized around the surface of the protein. Fig. 4 shows the surface pressure dynamics of ovalbumin at 0.1 and 1 M sodium phosphate ionic strengths. It appears that ionic strength does play a role in shielding the protein charge, but not until the post-induction regimes. The higher ionic strength solvent reduces the Debye length of charged protein side chains. This reduced charge-charge repulsion allows faster in-

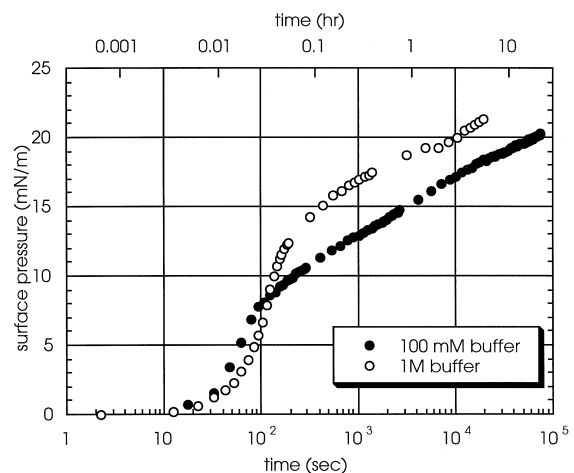


Fig. 4. Dynamic surface pressure of ovalbumin at the heptane/buffer interface at different buffer ionic strengths, pH = 7.1, protein concentration $C_b = 10 \mu\text{g/ml}$.

terfacial saturation and conformational changes as proteins fill the interface. Long time effects are similar between the two ionic strengths, further suggesting the importance of interfacial relaxation of adsorbed protein molecules.

3.2. β -Casein

β -Casein is a protein found in bovine milk that serves an important function in the stabilization and surface properties of the casein micelles. Considerable research on proteins is undertaken by the food processing industry, where characterization of the adsorption of various milk proteins is important in controlling the properties of cheese, homogenized milk, and other dairy emulsions. The caseins (α , β , and κ) comprise a family of proteins that lack significant amounts of ordered structure, in contrast to globular proteins which often exhibit regular secondary structures. β -Casein is a random coil protein of molecular weight 23 500, with a highly charged N-terminal sequence but distinctly hydrophobic character further down the peptide chain. Thus, it exhibits significant surface activity. The protein is believed to be disordered due to the complete absence of disulfide bonds and the rather large (17%) quantity of structure-breaking proline side chains.

The time-dependent adsorption of β -casein is seen in Fig. 5, the transient interfacial tension of various concentrations of β -casein at the heptane/aqueous buffer interface. This protein shows more rapid adsorption dynamics than ovalbumin and the ability to attain an apparent equilibrium interfacial tension (~ 19 mN/m). A diffusional induction period in tension relaxation is also seen in this system at a protein concentration below 10 $\mu\text{g}/\text{ml}$. The effects of protein depletion from the bulk solution are seen in the minimal tension changes at very low (1 $\mu\text{g}/\text{ml}$) bulk concentration. Considering the dimensions of a typical pendant drop (volume = 50 mm^3 , surface area = 70 mm^2), and cited values for monolayer β -casein surface concentration at hydrophobic interfaces (2–3 mg/m^2) [2], the 1 $\mu\text{g}/\text{ml}$ concentration provides no more than one-third of the protein molecules necessary to reach monolayer coverage

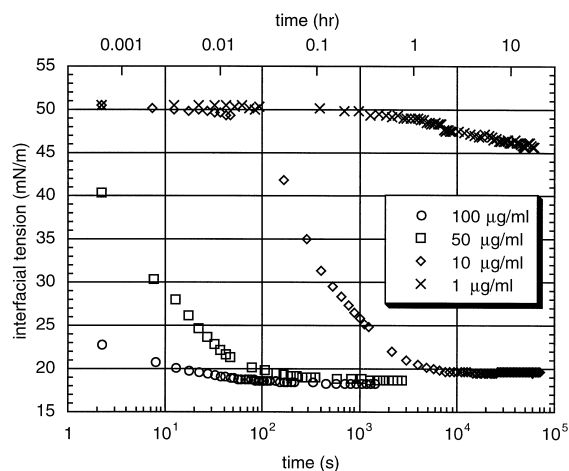


Fig. 5. Dynamic interfacial tension of β -casein at the heptane/aqueous buffer interface, pH = 7.1, 100 mM sodium phosphate buffer.

of the pendant drop. Thus, the tension does not significantly change over long periods. The slight reduction to 46 mN/m is attributed to these low coverages and to dilute impurities.

The tension dynamics of β -casein may be explained by the disordered structure of this protein in the bulk aqueous phase. It appears that the lack of regular structure promotes rapid adsorption and tension equilibration in the second and third regimes. This agrees with the hypothesis that slow interfacial unfolding and rearrangement of globular proteins dominates the tension kinetics beyond the induction regime. The flexibility of β -casein allows it to seek an equilibrium conformation sooner than an ordered globular protein. This may be due to the strong adsorption of the hydrophobic C-terminus, leaving the negatively charged 50 amino acid hydrophilic N-terminus suspended as loops and tails in the aqueous phase. These distinct variations in hydrophobicity localized at either end of the random-coil molecule cause β -casein to adsorb much like a typical surfactant. This hypothesis is in agreement with conclusions drawn from neutron reflectivity studies and NMR spectroscopy to β -casein adsorption at the oil/water interface [33]. However, the viscoelastic film that forms upon adsorption indicates that this protein is not a typical surfactant.

In comparing ovalbumin and β -casein data, it is apparent that the long time dynamics that are characteristic of ovalbumin adsorption at all concentrations are absent in the β -casein systems.

3.3. Lysozyme

Another globular protein studied in this work is lysozyme purified from chicken egg white. Lysozyme is a protective enzyme whose primary function is the hydrolysis of heteropolymers in bacterial cell walls. This common antibacterial agent is found in mucus and other protective body fluids, and also has medicinal applications in the treatment of ulcers, skin diseases, and post-operative infections. Lysozyme is a small globular protein (14 300 Da) with significant α -helix and β -sheet structures. The enzyme is positively charged at neutral pH (isoelectric point pH = 10.7) and has a significant dipole moment. It also forms head-to-tail associations in solution from specific interactions between Trp-62 and Glu-35 [34].

The interfacial tension dynamics of lysozyme at the heptane/buffer interface are shown in Fig. 6. Similar results to ovalbumin are seen, with a logarithmic decrease in the tension over long time scales. The low concentration plot exhibits characteristic globular protein behavior, most

noticeably a distinct slope discontinuity, possibly resulting from surface saturation, and transition to the long-time regime. Slow unfolding and rearrangement may again explain the continued relaxation of this globular protein over periods of several hours.

Lysozyme was also used to study the effects of urea denaturation on adsorption behavior of globular proteins. Similar to ovalbumin, lysozyme denaturation is induced at approximately 6 M urea and the protein is considered fully denatured at 9 M [35]. High concentrations of urea have been shown to alter slightly the far-UV circular dichroism spectra [36]. Crystal structures of lysozyme grown in the presence of various urea concentrations show distinct binding sites of individual urea molecules on the lysozyme molecule, but only subtle overall conformational changes [37]. Fig. 7 shows the dynamic surface pressure of 10 $\mu\text{g}/\text{ml}$ lysozyme at pH 7.1 at various urea concentrations. With results very similar to ovalbumin, the sharp shoulder in the dynamic pressure of the pure protein solution at the heptane/buffer interface is eliminated as urea concentration is increased. A weaker protein interfacial affinity in urea solutions may explain the slower intermediate time surface pressure increase. The urea-free solution reaches a surface pressure discontinuity at 11 mN/m and $t \sim 150$ s,

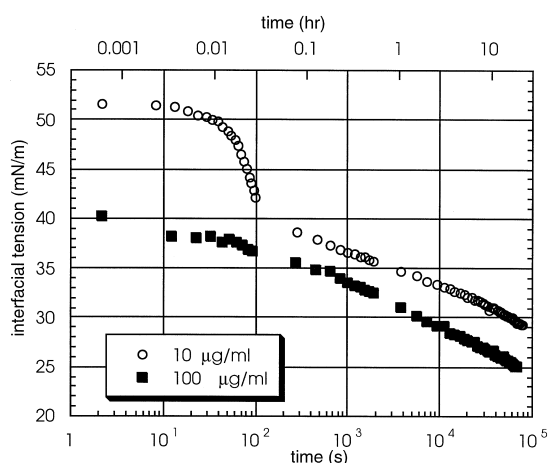


Fig. 6. Dynamic interfacial tension of lysozyme at the heptane/aqueous buffer interface, pH = 7.1, 100 mM sodium phosphate buffer.

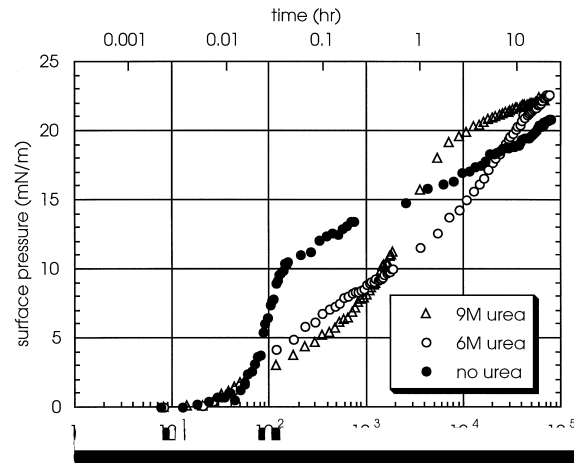


Fig. 7. Dynamic surface pressure of urea-denatured lysozyme solutions at the heptane/aqueous buffer interface. $C_b = 10 \mu\text{g}/\text{ml}$, pH = 7.1, 100 mM sodium phosphate buffer.

while the concentrated urea solutions require approximately 1500 s to reach this pressure. At longer times, extent of denaturation is again positively correlated to the rate of surface pressure increase, and the 6 and 9 M urea solutions achieve greater surface pressures than the pure protein system at 20 000 and 3000 s adsorption time, respectively.

3.4. Bovine serum albumin

A proposed mechanism for the development of strong interfacial films in certain proteins is non-native disulfide cross-linking [38]. Proteins with significant amounts of sulphhydryl groups in the form of cystine residues are thought to cross-link covalently when these reactive groups are exposed upon denaturation. Disulfide bond formation is believed to play a role in time-dependent β -lactoglobulin polymerization in tetradecane emulsions [39]. Chemical reduction of disulfide bonds using the reactive compound dithiothreitol [40] allows analysis of the effects of breaking these bonds on protein stability. DTT is often used to reduce the viscosity of protein-stabilized foams and aids in dough processing [2]. We hypothesize that addition of DTT to a protein rich in disulfides, such as bovine serum albumin (17 disulfide bonds), may significantly alter its stability and adsorption dynamics. However, the control experiment of DTT alone in phosphate buffer (Fig. 8) showed significant surface activity and long time dynamics indicative of polymerization of the reagent. It is likely that the free sulphhydryls in DTT react over long time scales, and thus make it difficult to isolate the effects of protein and DTT adsorption to the oil/water interface. Still, the dynamic tension of this protein in the absence of DTT allows one to investigate the importance of disulfide cross-linking on protein stability, aggregation, and gel formation.

Bovine serum albumin is a large globular protein (66500 Da) with good ion, fatty acid, and hormone binding capacities, found in bovine plasma. The primary function of this protein is the regulation of the colloidal osmotic pressure of blood. Fig. 9 shows the dynamic interfacial tension of low concentration BSA. Adsorption of this

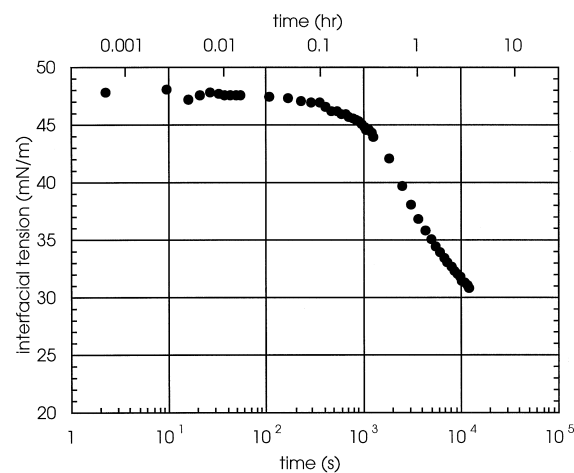


Fig. 8. Dynamic interfacial tension of 15 mM dithiothreitol at the heptane/aqueous buffer interface.

protein is similar to other globular proteins with distinct regimes indicated by marked slope changes. However, BSA exhibits a less dramatic shoulder between the second and third regimes than the other globular proteins, and does not form a visibly collapsible film at long times.

There is some contradiction in the explanation of the tension dynamics of BSA. One might expect that the high number of disulfide bonds in BSA is an indication of greater protein stability. However, the values from the tension dynamics

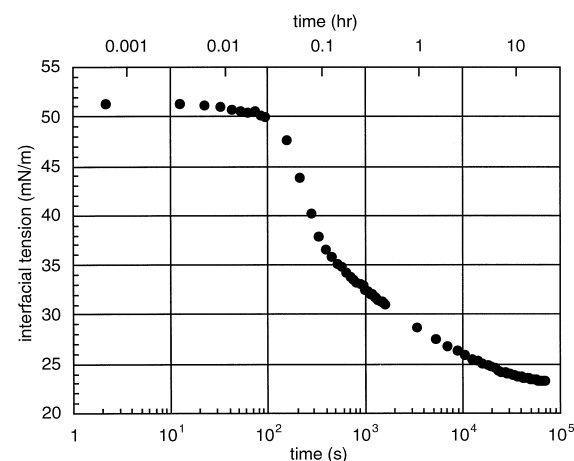


Fig. 9. Dynamic interfacial tension of bovine serum albumin at the heptane/aqueous buffer interface. $C_b = 10 \mu\text{g/ml}$, pH = 7.1, 100 mM sodium phosphate buffer.

suggest that BSA is highly surface active, achieving the highest surface pressure of the globular proteins studied (28 mN/m) after 10 h. It seems that the 17 disulfide bonds still permit the BSA molecule to orient itself in such way to achieve a high surface pressure. An alternative hypothesis that arises from the BSA information is that only minimal unfolding occurs upon adsorption, and that only small changes of these largely-globular adsorbed species are required to change the tensions at long times. This is certainly a viable explanation that may be best investigated through spectroscopic means.

3.5. Lipases

Interfacial phenomena of proteins are particularly important for the analysis of enzymes that are active at the oil/water interface. Lipases are a class of such enzymes that hydrolyze lipid structures, mobilizing them and directly affecting cell growth. Since the presence of these enzymes at the oil/water interface is necessary for their function, it is of interest to examine the dynamics of adsorption of these proteins and the effects of film formation on enzyme activity.

Lipase activity has been correlated with oil/water interfacial tension for porcine pancreatic lipase and human gastric lipase [41]. Surfactants were used to lower initially the interfacial tension, and assays of the water-soluble tributyrin hydrolysis products showed optimum lipase activities at interfacial tensions of 8–13 mN/m . However, it is difficult to determine whether the tension changes in these mixed systems were due to protein adsorption, protein/surfactant interaction, or substrate conversion.

3.6. Wheat germ lipase

The adsorption of lipase purified from wheat germ and the yeast *Candida rugosa* is studied here. Wheat germ lipase is an esterase that is active on triacetin and tributyrin, but inactive on longer chain triacylglycerols. It has the primary function of catalyzing initial steps in lipid mobilization, which eventually leads to germinative growth. Lipolysis by this enzyme commonly

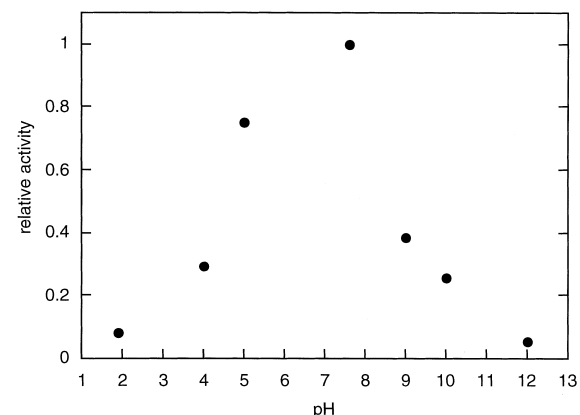


Fig. 10. Activity of wheat germ lipase on triacetin as a function of pH relative to maximum activity ($6.73 \mu\text{eq. fatty acid liberated/mg lipase/h}$) at pH 7.6. From Rajendran et al. [43] and Rao et al. [44].

causes rancidity of cereals, making them unsuitable for human consumption and thus prompting research in agricultural and food chemistry fields [42].

Wheat germ lipase has a molecular weight of 42 000, is ellipsoidal in shape, and contains 20% α -helix, 40% β -sheet, and the balance random coil structure at neutral pH. Previous studies have confirmed significant conformational changes in the acidic ($\text{pH} = 3.0$) and alkaline ($\text{pH} = 12.0$) regions that are accompanied by loss of activity, as shown in Fig. 10 [43,44]. Gross conformational changes occur at extremes of pH as observed by circular dichroism, including loss of α -helical structure and aggregation.

3.7. *Candida rugosa* lipase

Another lipase with significantly higher activity than that isolated from wheat germ was also studied. *Candida rugosa* lipase catalyzes the hydrolysis of triacylglycerol to diacylglycerol and a fatty acid anion. The activity of this enzyme has been widely studied due to its ability to liberate all lengths of acyl chains, regardless of their location in a glycerol [45], making it an attractive alternative to the harsh conditions needed to synthesize chemically fatty acids. Under similar conditions, *C. rugosa* lipase is approximately 80

times more active than wheat germ lipase, and has the ability to degrade olive oil triglycerides unlike the wheat germ enzyme [46].

C. rugosa lipase is a larger molecule than wheat germ lipase, with a molecular weight of 57 kDa, an isoelectric point of pH = 4.7, and two disulfide bonds. This enzyme has significant secondary structure, with a high aliphatic index and good stability in solution. The activity kinetics of this enzyme show little inhibitory effect of glycerol, a primary substrate. Virto et al. [47] report the addition of organic solvents to the reaction emulsion shows a decrease in activity with increasing polarity of the solvent, with a maximum enzyme stability in 20% isoctane. This stability suggests that immediate denaturation at the oil/water interface does not occur.

By comparing the tension dynamics and film formation of lipases to other globular proteins, we can determine if the interfacial activity of these enzymes renders them more resistant to adsorption and gelation. Following the assumption that adsorption involves at least partial denaturation and eventual aggregation, we can also draw correlations between interfacial- and pH-induced aggregation of this protein. Since loss of structure and aggregation accompany loss of activity at extremes of pH for wheat germ lipase, we speculate that the formation of a collapsible gel in these systems after prolonged contact with an oil interface may also suggest loss of activity.

Fig. 11 shows the dynamic interfacial tension of 10 µg/ml solutions of wheat germ and *Candida rugosa* lipase at the heptane/aqueous buffer interface. Induction periods are approximately the same for both proteins. The general long-time trends are similar to other globular proteins, with reduction of the interfacial tension likely attributed to continued conformational changes. It appears that, while active at oil interfaces, these enzymes may not be significantly more stable than other globular proteins when they encounter the heptane phase. Comparison of the two enzymes indicates that *Candida rugosa*, the more active enzyme, has a lower rate of interfacial tension reduction and lower long-time surface pressure in the later regimes. This suggests that the structure of *C. rugosa* lipase resists interfacial

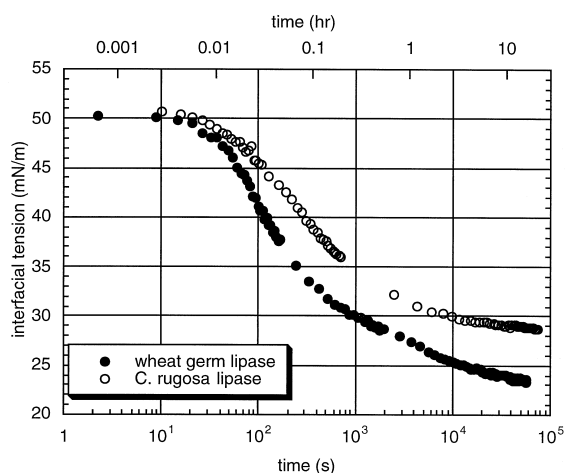


Fig. 11. Dynamic interfacial tension of lipases from wheat germ and *Candida rugosa* at the heptane/aqueous buffer interface. $C_b = 10 \mu\text{g}/\text{ml}$, pH = 7.1, I = 100 mM phosphate buffer.

denaturation better than the wheat germ lipase, thereby allowing it to retain a greater activity. The low dynamic tension values for wheat germ lipase may be correlated with the dramatic loss of regular conformation and activity of this enzyme at extremes of pH.

3.8. Glutamate dehydrogenase from the thermophile *P. furiosus*

Thermophiles are a class of organisms characterized by the ability to survive under unusually high temperatures. Enzymes purified from thermophiles have evolved to remain active at the high temperatures and pressures found in volcanically heated geothermal waters, and deep-sea and surface hot springs. Activity is typically seen in the range of 40–80°C [48], and in some cases above 100°C. This suggests that thermophilic enzymes have very stable protein structures. Accordingly, it is of interest to examine these proteins to determine if the high resistance to thermal denaturation corresponds to a resistance to interfacial denaturation upon adsorption to the oil/water interface.

Pyrococcus furiosus is a marine hyperthermophilic bacterium that grows optimally at 100°C [49]. Glutamate dehydrogenase from *P. furiosus* is

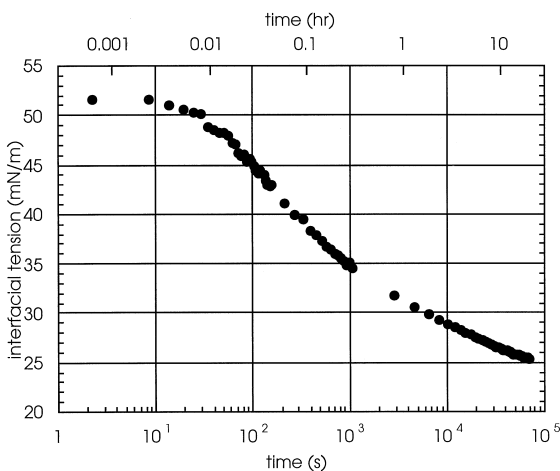


Fig. 12. Dynamic interfacial tension of *Pyrococcus furiosus* glutamate dehydrogenase at the heptane/aqueous buffer interface. Protein concentration $C_b = 10 \mu\text{g/ml}$, pH = 7.1, I = 100 mM phosphate buffer.

a medium-sized enzyme subunit (47000 Da) of a hexamer that is activated at 40°C and begins thermal denaturation at 110°C. This enzyme has a high percentage of buried hydrophobic groups, and is believed to be additionally stabilized by ion-pair networks on the surface of the subunits [50].

Recombinant GDH was used for adsorption experiments. Fig. 12 shows the dynamic interfacial tension of *P. furiosus* GDH at the heptane/buffer interface. A similar delay is observed in this low concentration system to that for mesophilic proteins, followed by the characteristic tension reductions of the second and third regimes. Long time dynamics similar to other globular proteins are observed, with slow reduction of tension as the protein forms a viscoelastic film at the interface.

The similarities in the adsorption dynamics of glutamate dehydrogenase from the hyperthermophile *Pyrococcus furiosus* to other globular proteins suggests that activity maintenance at high temperatures is not indicative of a native protein structure resistant to adsorption and denaturation at the oil/water interface. It appears that the order/disorder transition induced by the non-polar phase is of greater destabilizing magnitude than is thermally-induced denaturation. Slowly-

increasing surface pressures, similar to other globular proteins at extended times, and the visible collapse of GDH films indicates that the gelation phenomena is also seen in this system.

4. Discussion

4.1. Regimes of dynamic interfacial tension

At dilute protein concentrations ($\sim 10 \mu\text{g/ml}$), the dynamic interfacial tension can be divided into three time regimes that are typical for many proteins. These regimes are illustrated in Fig. 13 for a hypothetical case. The first is an induction regime, where the interfacial tension remains relatively constant at the pure fluid values. Regime II is characterized by a sharp decline in tension from this initial value. The final regime is a steady decline in interfacial tension, at a less negative slope than Regime II on a semi-log plot. The slow tension reduction defined by the third regime often extends for several hours. We describe each of these regimes.

4.2. Regime I: induction

The first regime seen in the interfacial tension experiments is an induction time where the tension is that of the pure solution. This phenomenon has been frequently observed for adsorption of low-concentration protein solutions at the air/water interface [4,5,51,52]. Some authors at-

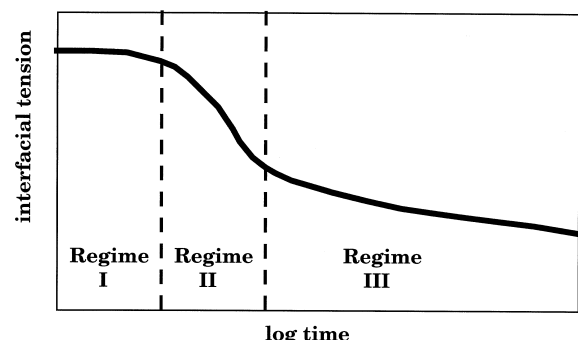


Fig. 13. Typical dynamic interfacial tension response of protein in dilute aqueous solution adsorbing to the oil/water interface.

tributed this lag time to the tensiometry method used [17,53], citing expansion of the interface due to initial protein adsorption and tension lowering for drop volume and pendant drop methods. However, experiments employing static interfaces or the Wilhelmy plate method have also noted a lag time, sometimes as long as several hours [5,16]. Furthermore, radiotracer and ellipsometric techniques have indicated that the surface concentration does not exhibit this lag at early times [5,6,16]. Thus, at early times and low protein concentrations, molecules are present at the interface, but do not appreciably reduce the interfacial tension. It is likely that this anomalous behavior extends to protein adsorption at the oil/water interface, which also exhibits an induction period in dynamic tension.

In comparing the dynamic surface and interfacial tensions of dilute ($10 \mu\text{g/ml}$) ovalbumin solutions at the aqueous/air and aqueous/heptane interfaces, an immediate observation is the variation in induction time for ovalbumin adsorption at either interface (Fig. 14). Two orders of magnitude difference exists in the induction period for the same protein solution. The lag time to achieve a surface pressure of 1 mN/m is $\sim 10 \text{ s}$ for adsorption at the heptane/water interface and over 1000 s at the air/water interface. The entire

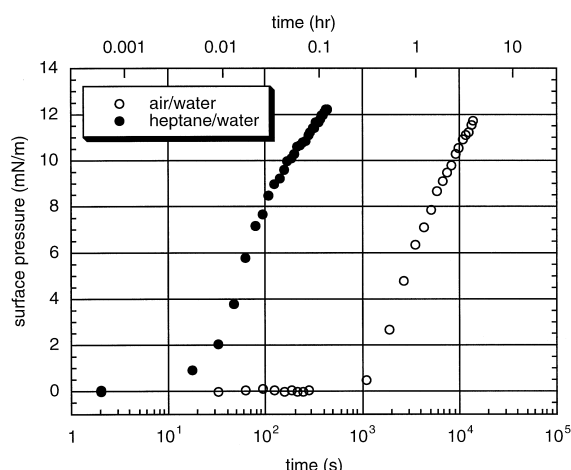


Fig. 14. Dynamic interfacial and surface tension of ovalbumin adsorbed at the heptane/water and air/water interfaces. Protein concentration $10 \mu\text{g/ml}$, $\text{pH} = 7.1$, 100 mM sodium phosphate buffer.

surface pressure response appears quite similar for both cases except for the shift in time scale, illustrating the characteristics of the non-polar phase.

This difference in the induction regime suggests possible mechanisms for initial protein adsorption at the oil/water interface. For dilute solutions, diffusion of protein molecules to the interface is important at early times. The effects of diffusion on surface concentration of an adsorbing species is predicted using the equation of Ward and Tordai [54]

$$\Gamma(t) = 2C_b \sqrt{\frac{Dt}{\pi}} \quad (2)$$

$\Gamma(t)$ is the interfacial concentration, C_b is the bulk protein concentration, and D is the diffusion coefficient. This equation has been simplified under the assumption that back diffusion, a result of reversible adsorption, is negligible. If we directly apply this equation for the dilute ovalbumin solution ($C_b = 10 \mu\text{g/ml}$), using a typical protein diffusion coefficient of $5 \times 10^{-7} \text{ cm}^2/\text{s}$, we find that diffusion of a full monolayer of protein to the interface ($\Gamma = 2-3 \text{ mg/m}^2$) [2,4] requires approximately 600 s. This value lies between the induction times seen at the oil and air interfaces. Since full monolayer coverage is a conservative estimate for the coverage necessary to induce tension declines, the longer experimental induction time seen at the air/water interface requires further analysis. We propose that proteins at the air/water interface may exhibit reversible adsorption to a larger extent than those exposed to an oil/water interface. Hydrophobic residues on the protein have a greater affinity for the oil interface than the air interface, and are more strongly adsorbed at the former. This effect is probably mediated by both surface hydrophobicity and conformational stability of the protein, in agreement with the explanation of Wei [21] for adsorption at the air/water interface.

This is supported using simple adsorption dynamics arguments. To address the issue of surface pressure increases with increased interfacial coverage, we look to a surface equation-of-state. For simplicity, we combine the well-known Langmuir

adsorption isotherm with the Gibbs' equation to yield the common result

$$\Pi(t) = -k_B T \Gamma_{\max} \ln \left(1 + \frac{\Gamma(t)}{\Gamma_{\max}} \right) \quad (3)$$

where Π is the surface pressure, k_B is Boltzmann's constant, T is the temperature, and Γ and Γ_{\max} are the molecular surface concentration (protein molecules/area) at time t and at maximum coverage, respectively. Γ_{\max} may be considered the inverse of the projected area of an adsorbing molecule. This equation is used to compare protein molecules ($1/\Gamma_{\max} = 2000 \text{ \AA}^2$) with typical low-molecular weight surfactants ($1/\Gamma_{\max} = 20 \text{ \AA}^2$) as shown in Fig. 15. There is a marked effect of the molecular size of the adsorbing material on the surface pressure, with large spheroids the size of protein molecules requiring over 99% of monolayer coverage before surface pressures of 1 mN/m are seen. It is apparent that the number of surface contacts plays a major role in surface pressure of a fluid interface, and suggests a possible explanation for why proteins exhibit an induction period in their surface tension dynamics.

The differences in induction periods for a pro-

tein solution of the same concentration adsorbing at the oil and air interfaces implies a difference in affinity and denaturation kinetics at these interfaces. Thus, it is instructive to consider diffusion-controlled adsorption under the assumption that the change in free energy of a protein between a bulk and adsorbed state directly affects the kinetics of unfolding and subsequent surface pressure increase. We assume from Fig. 14 that the oil phase has a greater free energy of adsorption, thereby inducing more rapid denaturation and earlier interfacial tension declines than the air interface. This effect may be manifested in a larger equilibrium constant for adsorption at the oil interface. For simplicity, an examination of the early time kinetics of surfactant adsorption as a function of the adsorption rate constant is repeated here using a linear adsorption isotherm

$$\Gamma = KC \quad (4)$$

where K is the net adsorption constant with units of length and C is the bulk protein concentration. This isotherm is of limited practical applicability, but illustrates the effect of affinity of adsorption on dynamics of surface concentration changes. Sutherland [55] provides the time-dependent solu-

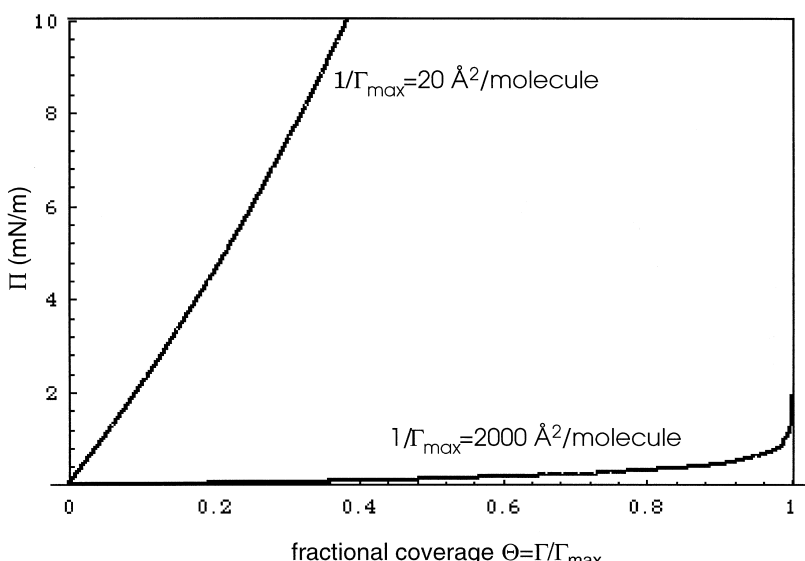


Fig. 15. Surface equation of state using a Langmuir adsorption model at 298 K. Surface pressure of an adsorbed film as a function of fractional coverage is highly dependent on size of adsorbing species.

tion to diffusion to an interface with linear adsorption

$$\Gamma = \Gamma_{\text{eq}} \left[1 - \exp\left(\frac{Dt}{K^2}\right) \operatorname{erfc}\left(\frac{\sqrt{Dt}}{K}\right) \right] \quad (5)$$

Γ_{eq} is the equilibrium surface concentration (KC_0) and D is the diffusion coefficient. This equation reduces to Eq. (2) at short times and large values of K . Using typical values for the protein systems studied in this chapter ($D = 5 \times 10^{-7} \text{ cm}^2/\text{s}$, $C_0 = 10 \mu\text{g/ml}$), a plot of the dynamic surface coverage for different values of K is shown in Fig. 16. As expected, large adsorption equilibrium constants favor more rapid initial increases in surface concentration and longer times to approach equilibrium. The observed induction periods may result from differences in the rate of adsorption arising from the nature of the hydrophobic phase. This adsorption rate may be considered a measure of the conformational stability and denaturation kinetics of the protein at the interface, which is probably related to the free energy of adsorption. The shape of the curves suggests that proteins at the air/water interface, if described by a low equilibrium adsorption con-

stant, may not achieve a high enough surface concentration to change noticeably the surface tension over a period of several hours, a phenomenon that has been observed previously [21]. However, the same proteins may be strongly adsorbed at an oil boundary.

The oil/water interface exhibits short induction periods. Since the aqueous protein diffusion rates should be equal regardless of the second phase, it is clear that heptane directly effects the interfacial adsorption of proteins and the subsequent changes in surface pressure. Fig. 17 shows a schematic of this regime for proteins adsorbing to the oil/water interface. At dilute aqueous concentrations, characterized by a small number of molecules at the interface, strongly adsorption arises from the presence of surface hydrophobic groups, and conformational changes occur. Unfolding of the protein exposes new residues to the oil phase, which also adsorb due to the similarities in environments of the oil phase and interior of the protein molecule. Surface pressure changes remain negligible until a sufficient number of residues adsorb. Once a critical surface concentration of adsorbed side chains is reached, the dynamic tension profile moves to Regime II.

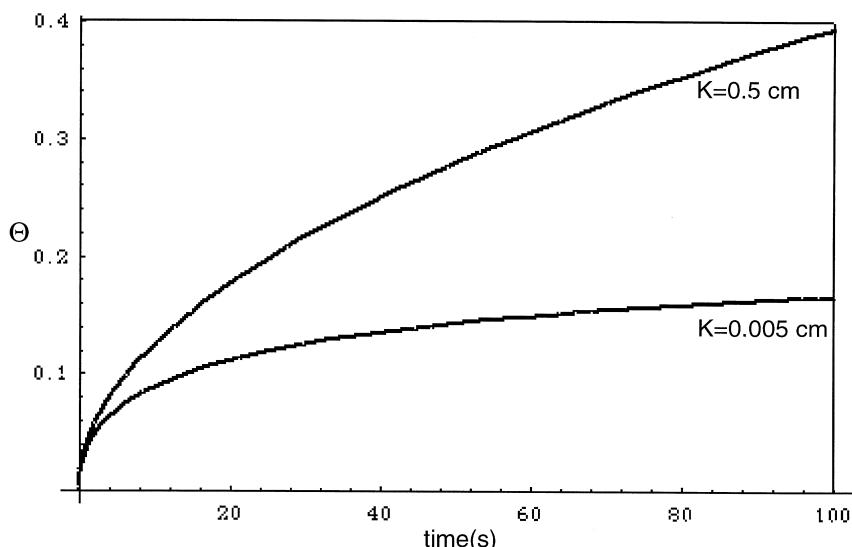


Fig. 16. Dynamic surface coverage at early times during diffusion controlled adsorption using a linear adsorption isotherm $\Gamma = KC$. $D = 5 \times 10^{-7} \text{ cm}^2/\text{s}$, $C_0 = 10 \mu\text{g/ml}$. Large adsorption rate constant results in faster increase in surface concentration. Small adsorption constant reaches a lower apparent equilibrium surface concentration sooner.

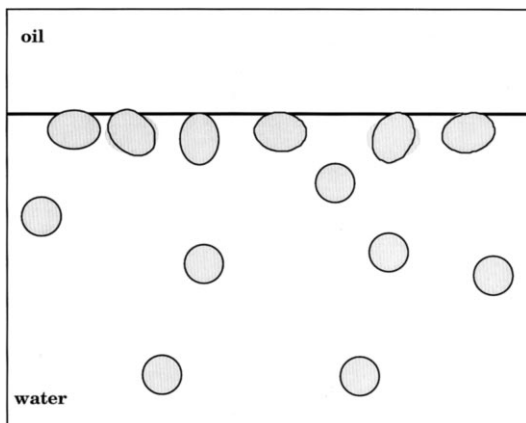


Fig. 17. Schematic of globular protein adsorption at the oil/water interface in Regime I of dynamic interfacial tension. Induction period characterized by diffusion of proteins to the interface and initiation of conformational changes of adsorbed proteins. Native conformation proteins represented as circles; ellipses indicate conformational changes.

It should be stressed that the induction period only exists for very dilute protein solutions. For concentrated solutions, interfacial tension dynamic curves at the oil/water interface proceed to Regime III faster than the time scale measurable using the pendant drop technique. In these cases, we are unable to measure diffusional effects, and only observe the steady decline in tension characteristic of the third regime in Fig. 13. Within the first few seconds of creation of an oil/water interface, we estimate that high bulk protein concentration results in an interfacial concentration of protein molecules above the critical value necessary to induce tension declines. The absence of a lag period at high concentrations at the air/water interface has also been noted. We explain further the third regime in tension dynamics later in this section.

4.3. Regime II: monolayer saturation

Beyond a certain concentration of adsorbed species, a steep decline in the interfacial tension is observed and continues for several seconds. As the interface becomes more saturated with protein, changes in both the surface concentration and interfacial tension are seen. A schematic of

Regime II is shown in Fig. 18. Continued loading of the interface may be achieved by two methods. Adsorbed proteins relaxing from their rigid conformations allow new side chains from the interior of the protein to adsorb, increasing the number of contacts between the protein and oil phase. This phenomenon may be the onset of irreversible adsorption for a protein molecule. The other method of surface saturation in this regime is the diffusion of new proteins from the bulk aqueous phase. Both routes increase the number of adsorbed entities, thereby decreasing the interfacial tension over time. Considering the induction period explanations of Regime I, one may suspect that the conformational changes and denaturation of adsorbed proteins are more important in tension reduction than initial diffusion and adsorption. If this is the case, Regime II may be an indication of the conformational stability of adsorbed proteins, i.e. a measure of the kinetics of interfacial unfolding.

Conformational changes of adsorbed proteins may provide a new environment for bulk proteins that approach the initial adsorbed layer. If this layer results in attractive interactions between adsorbed and bulk molecules, additional layers begin to form at the interface. We have seen from area compression and electron microscopy experi-

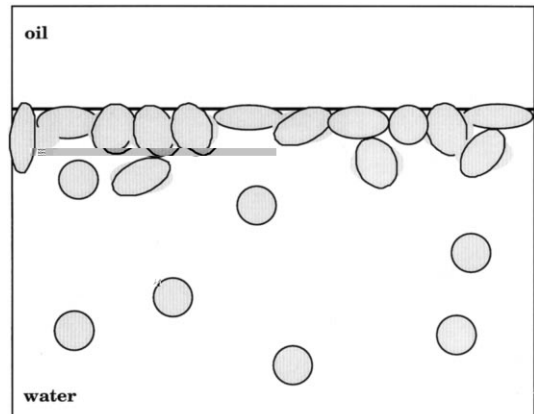


Fig. 18. Schematic of globular protein adsorption at the oil/water interface in Regime II of dynamic interfacial tension. Interface becomes filled with protein molecules which relax into less compact structures, causing declines in interfacial tension. Formation of multilayers may also be initiated.

ments that a viscous layer that exhibits mechanical strength forms as a result of protein adsorption at the oil/water interface. These results are suggestive of multilayer formation. The aggregation of new molecules to previously adsorbed proteins may be initiated in this regime, and have an effect on the tension dynamics as well. Thus, many factors may effect the rapid decline in interfacial tension after the induction period, making prediction using traditional theories difficult. For our experiments, we analyze the slope of this region to attempt to correlate it to known values of bulk conformational stability. This will determine if stability is important in this regime and if bulk and interfacial protein stability are related.

4.4. Regime III: interfacial gelation

The final regime is a slow decline in tension attributed to conformational changes of the adsorbed layer, and continued building of a gel-like network. Fig. 19 shows a schematic of this regime. Adsorbed molecules in the initial layer continue to change conformation in response to favorable environments for both hydrophobic and hydrophilic side chains. Lateral overlap and entanglement of this layer occurs (represented, for simplicity, as overlapping ovals in Fig. 19), as the molecules seek more energetically favorable conformations. Multiple layers build into the water phase, as proteins aggregate and form branches. These branches connect at various points, and further aggregation is promoted as adsorbed protein molecules slightly change conformation. The result is an amorphous gel-like network structure at the interface.

At extended times, the $\Pi-\Gamma$ surface equation-of-state for proteins is quite different from that of low molecular weight surfactants. In the latter case, molecular reorientation is very rapid ($< 10^{-3}$ s) [56]. Thus, the surface pressure is completely determined by the surface concentration over the time scales investigated, where equilibrium is established between adjacent adsorbed surfactants even before equilibrium is established with the bulk phase. This is not the case with macromolecules, and proteins in particular. Long-time molecular rearrangements, breakage and forma-

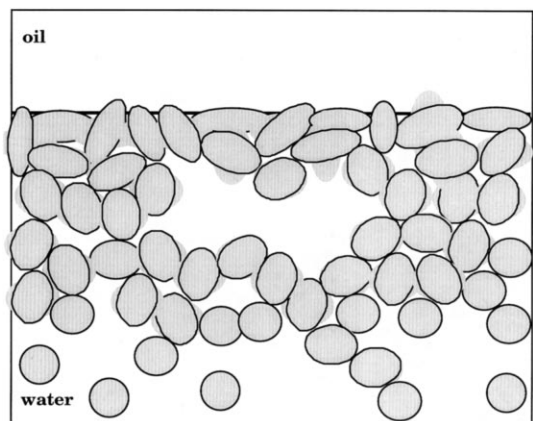


Fig. 19. Schematic of globular protein adsorption at the oil/water interface in Regime III of dynamic interfacial tension. Continued conformational changes of initial adsorbed layers and aggregation promote slow declines in tension over extended periods of time. Aggregate branching forms amorphous network structure.

tion of non-covalent structure-stabilizing bonds, and interactions between adjacent proteins continue to contribute to surface pressure changes, even when increases in the surface concentration cease. These continuing changes in conformation expose a new environment for protein molecules that subsequently approach the interface, leading to aggregation and the formation of a viscous, gel-like phase. This process is irreversible, and probably results in permanent loss of structure and enzymatic activity.

In many cases, the interfacial tension in the third regime exhibits a logarithmic-dependence on time. While the difficulties in theoretically predicting such a dependence are implied earlier, the linear response seen on the tension/log time plots may be indicative of gel-forming propensity of the adsorbed protein. Thus, our analysis involves comparison of the slope of this regime to structural characteristics of the protein to attempt to determine any correlations.

4.5. Discussion of dynamic interfacial tension results

Our experimental results indicate that at neutral pH, proteins adsorb at an oil/water interface and reduce the interfacial tension over time. For

the most part, similar time regimes are observed, regardless of protein enzymatic function. In order to understand better some of the driving forces for adsorption, we conduct a closer examination of the surface pressure dynamics and protein chemical and structural characteristics. Factors such as protein size, hydrophobicity, instability, charge, and disulfide bonds are considered in determining trends among the different proteins studied.

Six proteins were analyzed using several criteria obtained from the online SWISS-PROT database (<http://expasy.hcuge.ch>). This database compiles sequence, crystallographic, functional, and other structural information for biomolecules. Molecular weight, number of disulfide bonds, and percent hydrophilic amino acid residues are directly obtained from sequence information. In addition, an instability index and aliphatic index are calculated for each protein based on the following criteria.

The instability index is a measure of the relative likelihood of a protein to become denatured based on specific structural information. Guruprasad et al. [57] have identified certain dipeptides that are significantly more common in unstable proteins. A weighting system is constructed for several hundred dipeptides based on their occurrence in unstable proteins, allowing for the statistical calculation of an instability index for any protein sequence. An instability index below 40 indicates a stable structure.

Surface hydrophobicity of proteins likely plays a role in the interfacial tension dynamics at the oil/water interface. Kato et al. [58] determine the hydrophobicity of several proteins using the fatty acid fluorescent probe *cis*-paranarcic acid. In addition, emulsifying activity of proteins in stabilizing corn oil emulsions are determined by the turbidimetric method of Pearce and Kinsella [59]. These two indices are reported for three of the proteins examined here. Another method to determine the effective surface hydrophobicity of proteins is hydrophobic interaction chromatography (HIC). Tripp [25] reports the retention times of several proteins, with longer times indicating higher surface hydrophobicity. HIC values for β -casein,

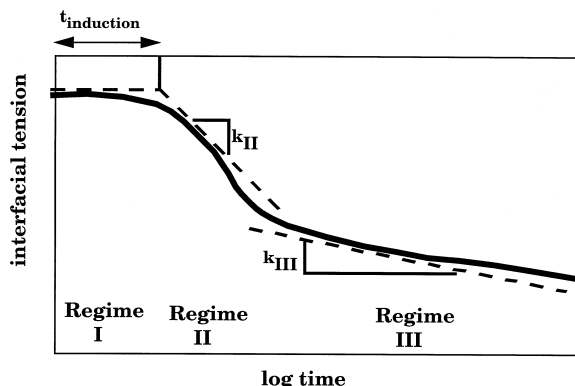


Fig. 20. Typical interfacial tension dynamics of protein adsorption at the oil/water interface showing methods of quantifying each regime. Induction time of Regime I determined by extrapolating slope from Regime II to zero surface pressure. Slopes of Regimes II and III show logarithmic dependence of tension on time.

BSA, and lysozyme are used here as another comparison criterion.

These indices are used to draw correlations between protein bulk structural information and the interfacial tension dynamics. The three regimes of tension dynamics are quantified as shown in Fig. 20. The length of the induction time defined as Regime I is obtained by determining the slope of Regime II and extrapolating to the $t = 0$ interfacial tension. The apparent logarithmic dependence of tension on time in Regimes II and III suggests the form

$$\sigma(t) \sim k_{II} \log(t)$$

$$\sigma(t) \sim k_{III} \log(t) \quad (6)$$

to describe these regimes. A logarithmic curve fit is applied to the tension data, and the resulting slope on the semilog plot is reported as k_{II} and k_{III} .

Table 1 shows the values of structural criteria, dynamic tension analyses at 10 $\mu\text{g}/\text{ml}$ protein concentration, and 10-h surface pressure for β -casein, bovine serum albumin (BSA), *Candida rugosa* lipase, ovalbumin, *Pyrococcus furiosus* glutamate dehydrogenase, and lysozyme. The pro-

Table 1
Individual characteristics and dynamic adsorption values for six of the proteins studied

Protein	Molecular weight ^a	Disulfide bonds ^a	Instability index ^a	Surface hydrophobicity ^b	Emulsifying activity ^b	HIC retention (min) ^c	Regime I induction time (s)	Regime II slope (k_{II}) (mN/m/log(s)) $\sigma \sim k_{II} \log(t)$	Regime III slope (k_{III}) (mN/m/log(s)) $\sigma \sim k_{III} \log(t)$	Π (mN/m) at 10 h
β-casein	23 583	0	96.62	—	—	∞	80	-27.3	0.0	30
BSA	66 432	17	40.11	1400	160	6.7	119	-28.0	-7.2	28
<i>C. rugosa</i> lipase	57 094	2	37.31	—	—	—	31	-10.6	-1.8	26
Ovalbumin	42 749	1	37.18	60	58	—	29	-13.9	-4.1	20
<i>P. furiosus</i> GDH	47 114	0	31.34	—	—	—	25	-10.5	-4.5	24
Lysozyme	14 313	4	16.09	100	56	18	44	-24.1	-3.8	20

^a From SWISS-PROT database.

^b From [58,59].

^c From [12].

teins are in order of increasing stability as measured by the instability index.

Induction times for the proteins studied show little variation, from approximately 25 to 120 s. Previously, we explain Regime I as chiefly diffusion-controlled, with higher protein concentrations showing no induction period. However, a distinct difference in the induction times for protein adsorption at the oil/water and air/water interfaces suggests that an initial equilibrium adsorption constant is important as well. We relate this apparent constant to the initial strength of adsorption and the ease of interfacial denaturation, with high values indicating strong adsorption (oil > air). When the protein (instead of the external phase) is varied, these adsorption tendencies are likely related to the protein surface hydrophobicity and conformational stability, two parameters that characterize the different proteins as seen in Table 1. However, in examining the data, no reasonable arguments can be made to correlate structural information with duration of induction at the oil/water interface. Larger values of surface hydrophobicity seen in BSA and β -casein appear to be correlated to longer induction times. This seems unlikely, since a greater hydrophobicity of the protein should shorten the induction time. Since all induction periods occur in the first 2 min at the oil/water interface (compared to several hours at the air/water interface), we hesitate to attribute lag times to specific structural characteristics. Thus, over the time scales measurable using the pendant drop technique, the effect of the oil phase on a protein in solution is so strong that it appears to level the playing field when describing the early dynamic tension behavior of the different proteins studied here.

Regime II is characterized by continued diffusion, conformational changes of adsorbed proteins, and initiation of the gelation phenomenon. Beyond a critical interfacial concentration, tension declines rapidly as adsorbed proteins expose new groups to the oil phase. Faster rates of decline are indicated by larger negative k_{II} values. During this period, several correlation's are apparent.

First, protein surface hydrophobicity is directly related to the rate of tension decline in Regime II. BSA and β -casein display the greatest rates of tension decline, and have high values of surface hydrophobicity by the fluorescence or HIC methods. The results for lysozyme are less clear due to the conflicting surface hydrophobicity data. Ovalbumin, a less surface hydrophobic protein, has a k_{II} value only half as large as either of these proteins. These results indicate the importance of surface hydrophobicity on strong, irreversible adsorption as well as on the onset of gelation.

Second, the bulk stability of the protein may also be relevant. The random coil structure of the β -casein molecule is highly unstable in the bulk, which helps promote a rapid decline in tension due to easy conformational rearrangements in the interface. After exposure to an oil phase, however, β -casein attains a more stable adsorbed state. Ovalbumin, wheat germ lipase, and the thermophilic enzyme have low instability indices and small slope values, indicating that stability may hinder tension declines. Again, conclusions regarding lysozyme are difficult to draw. Although it is the most stable protein, it has a large k_{II} value. Perhaps the large HIC value of lysozyme indicates that surface hydrophobicity dominates the tension dynamics of this protein. This would suggest that lysozyme adsorbs strongly, but retains a more compact structure. In addition, the smaller molecular weight of lysozyme may allow the protein to pack more efficiently at the interface.

In the final regime, proteins continue to change slowly their conformation and build a viscoelastic interfacial film. This hypothesis is supported by the experimental data. k_{III} values for all globular proteins are larger than that for β -casein, a random coil protein. Greater protein stability seems to promote the long time dynamics of interfacial tension reduction. In β -casein, these dynamics are essentially absent. Surface hydrophobicity becomes less important in Regime III, as conformational changes in both the initial layer as well as the network branches (promoting further aggregation) determine the interfacial tension.

5. Conclusions

We have examined the adsorption dynamics of a set of several different proteins encompassing a representative sample of bulk structures and their stabilizing forces. Pendant drop tensiometry indicates that dilute protein solutions exhibit distinct regimes in their time-dependent interfacial tension with heptane. Interfacial tension dynamics are often seen over extensive periods of time, indicating the approach to adsorption equilibrium is not a fast process.

The various techniques used in this study provide a basis for speculation on the mechanism of protein adsorption. Initial protein adsorption is induced by hydrophobic interactions between the oil and surface hydrophobic protein residues. The non-polar oil phase at the interface aids in an order/disorder transition in the globular protein molecule, permitting significant unfolding of the protein. The fluidity of the oil/water interface facilitates this process, allowing sequestration of polar and non-polar side chains in their respective phases. Higher levels of protein structure help dictate the rate of unfolding, with random coil proteins able to achieve a relaxed conformation faster than globular proteins. The size and amphiphilicity of the protein, the contrast in polarity of the phases, and the flexibility of the fluid/fluid interface combine to render the adsorption irreversible.

The initial adsorption layer provides a foundation for further adsorption and aggregation. Proteins diffusing to this layer encounter an environment very different to their bulk surroundings. Interactions between foundation layer hydrophobic groups that were sterically hindered from orienting themselves in the oil phase and surface hydrophobic groups of diffusing proteins promotes further adsorption and unfolding. Large strands of aggregated protein form over a period of time, strengthening the adsorbed layer and leading to a condensed-gel phase. The degree of unfolding of each newly adsorbed protein decreases with distance from the interface as the gel pore sizes increase. Eventually, proteins diffusing to the adsorbed layer encounter an environment very similar to the bulk, and net adsorption ceases.

Acknowledgements

This work was supported by US DOE Grant DE-FG03-94ER14456. The algorithm used to fit an exact solution of the Young–Laplace equation to the edge coordinates of a pendant drop was kindly provided by Dr Harris Wong. Dr Wong's code was used in conjunction with the public-domain image processing software NIH-Image 1.59/pc to automate the experiment.

References

- [1] E. Dickinson et al., A neutron reflectivity study of the adsorption of β -casein at fluid interfaces, *Langmuir* 9 (1993) 242–248.
- [2] E. Dickinson, Recent trends in food colloids research, in: *Food Macromolecules and Colloids*, The Royal Society of Chemistry, Dijon, France, 1994.
- [3] T. Cosgrove, J.S. Phipps, R.M. Richardson, Neutron reflection from a liquid/liquid interface, *Colloids Surf.* 62 (1992) 199–206.
- [4] D.E. Graham, M.C. Phillips, Proteins at liquid interfaces. II. Adsorption isotherms, *J. Colloid Interface Sci.* 70 (3) (1979) 415–426.
- [5] J. Benjamins et al., Dynamic and static properties of proteins adsorbed at the air/water interface, *Faraday Discuss. Chem. Soc.* 59 (1975) 218–229.
- [6] B.W. Morrissey, C.C. Han, The conformation of β -globulin adsorbed on polystyrene latices determined by quasielastic light scattering, *J. Colloid Interface Sci.* 65 (3) (1978) 423–431.
- [7] D.G. Dalgleish, The conformations of proteins on solid water interfaces-caseins and phosvitin on polystyrene latices, *Colloids Surf.* 46 (2–4) (1990) 141–155.
- [8] E. Dickinson, B.S. Murray, G. Stainsby, Coalescence stability of emulsion-sized droplets at a planar oil–water interface and the relationship to protein film surface rheology, *J. Chem. Soc. Faraday Trans. I.* 84 (3) (1988) 871–883.
- [9] V.N. Izmailova, Structure formation and rheological properties of proteins and surface-active polymers of interfacial adsorption layers, in: D.A. Cadenhead, J.F. Danielli (Eds.), *Progress in Surface and Membrane Science*, Academic Press, New York, 1979, pp. 141–209.
- [10] C.W.N. Cumper, M.A. Alexander, Proteins at interfaces, *Rev. Pure Appl. Chem.* 1 (3) (1951) 121–151.
- [11] S. Ghosh, H.B. Bull, Adsorbed films of bovine serum albumin: tensions at air–water surfaces and paraffin–water interfaces, *Biochim. Biophys. Acta* 66 (1963) 150–157.
- [12] F. MacRitchie, A.E. Alexander, Kinetics of adsorption of proteins at interfaces. Part I. The role of bulk diffusion in adsorption, *J. Colloid Sci.* 18 (1963) 453–457.
- [13] F. MacRitchie, N.F. Owens, Interfacial coagulation of

- proteins, *J. Colloid Interface Sci.* 29 (1969) 66–71.
- [14] R.D. Bagnall, Adsorption of plasma proteins on hydrophobic surfaces. I. Albumin and β -globulin, *J. Biomed. Mater. Res.* 11 (1977) 947–978.
- [15] R.D. Bagnall, J.A.D. Annis, P.A. Arundel, A novel technique for studying the adsorption of plasma proteins on hydrophobic surfaces, *J. Biomed. Mater. Res.* 12 (1978) 653–663.
- [16] D.E. Graham, M.C. Phillips, Proteins at liquid interfaces. I. Kinetics of adsorption and surface denaturation, *J. Colloid Interface Sci.* 70 (3) (1979) 403–414.
- [17] A.J.I. Ward, L.H. Regan, Pendant drop studies of adsorbed films of bovine serum albumin. I. Interfacial tensions at the isoctane/water interface, *J. Colloid Interface Sci.* 78 (2) (1980) 389–394.
- [18] J.A. De Feijter, J. Benjamins, Adsorption kinetics of proteins at the air–water interface, International Symposium by the Food Chemistry Group of The Royal Society of Chemistry, The Royal Society of Chemistry, Leeds, 1986.
- [19] J. Castle et al., Mixed-protein films adsorbed at the oil–water interface, in: J.L. Brash, T.A. Horbett (Eds.), *Proteins at Interfaces. Physicochemical and Biochemical Studies*, American Chemical Society, Washington, D.C., 1987, pp. 118–135.
- [20] F. MacRitchie, Protein adsorption/desorption at fluid interfaces, *Colloids Surf.* 41 (1989) 25–34.
- [21] A.-P. Wei, J.N. Herron, J.D. Andrade, The role of protein structure in surface tension kinetics, in: D.J.A. Crommelin, H. Schellekens (Eds.), *From Clone to Clinic*, Kluwer Academic Publishers, The Netherlands, 1990, pp. 305–313.
- [22] A. Voigt et al., Axisymmetric drop shape analysis (ADSA) applied to protein solutions, *Colloids Surf.* 58 (1991) 315–326.
- [23] J.D. Andrade, V. Hlady, A.P. Wei, Adsorption of complex proteins at interfaces, *Pure Appl. Chem.* 64 (11) (1992) 1777–1781.
- [24] W. Van der Vegt, H.C. Van der Mei, H.J. Busscher, Interfacial free energies in protein solution droplets on FEP-Teflon by axisymmetric drop shape analysis by profile-IgG versus. BSA, *J. Colloid Interface Sci.* 156 (1993) 129–136.
- [25] B.C. Tripp, J.J. Magda, J.D. Andrade, Adsorption of globular proteins at the air/water interface as measured via dynamic surface tension: concentration dependence, mass-transfer considerations, and adsorption kinetics, *J. Colloid Interface Sci.* 173 (1995) 16–27.
- [26] W. Van der Vegt et al., pH dependence of the kinetics of interfacial tension changes during protein adsorption from sessile droplets on FEP-Teflon, *Colloid Polym Sci.* 274 (1996) 27–33.
- [27] S.-Y. Lin, K. McKeigue, C. Maldarelli, Diffusion-controlled surfactant adsorption studied by pendant drop digitization, *AIChE J.* 36 (12) (1990) 1785–1795.
- [28] R. Miller et al., Relaxation behaviour of human albumin adsorbed at the solution/air interface, *Colloids Surf. A* 76 (1993) 179–185.
- [29] R. Miller et al., Relaxation of adsorption layers at solution/air interfaces using axisymmetric drop-shape analysis, *Colloids Surf.* 69 (1993) 209–216.
- [30] P.E. Stein et al., Crystal structure of uncleaved ovalbumin at 1.95 Å resolution, *J. Mol. Biol.* 221 (1991) 941–959.
- [31] E. Tatsumi, N. Takahashi, M. Hirose, Denatured state of ovalbumin in high concentrations of urea as evaluated by disulfide rearrangement analysis, *J. Biol. Chem.* 269 (45) (1994) 28062–28067.
- [32] C.J. Beverung, C.J. Radke, H.W. Blanch, Adsorption dynamics of l-glutamic acid copolymers at a heptane/water interface, *Biophys. Chem.* 70 (1998) 121–132.
- [33] L.C. ter Beek et al., Nuclear magnetic resonance study of the conformation and dynamics of β -casein at the oil/water interface in emulsions, *Biophys. J.* 70 (1996) 2396–2402.
- [34] S.K. Banerjee, A.J. Pogolotti, J.A. Rupley, Self-association of lysozyme. Thermochemical measurements: effect of chemical modification of Trp-62, Trp-108, and Glu-35, *J. Biol. Chem.* 250 (20) (1975) 8260–8266.
- [35] Y. Maeda et al., Effective renaturation of reduced lysozyme by gentle removal of urea, *Protein Eng.* 8 (2) (1995) 201–205.
- [36] K.P. Barnes, J.R. Warren, J.A. Gordon, Effect of urea on the circular dichroism of lysozyme, *J. Biol. Chem.* 247 (6) (1972) 1708–1712.
- [37] A.C.W. Pike, K.R. Acharya, A structural basis for the interaction of urea with lysozyme, *Protein Sci.* 3 (1994) 706–710.
- [38] E. Dickinson, Structure and composition of adsorbed protein layers and the relationship to emulsion stability, *J. Chem. Soc. Faraday Trans.* 88 (1992) 2973–2983.
- [39] E. Dickinson, Y. Matsumura, Time-dependent polymerization of beta-lactoglobulin through disulphide bonds at the oil–water interface in emulsions, *Int. J. Biol. Macromol.* 13 (1) (1991) 26–30.
- [40] W.W. Cleland, Dithiothreitol, a new protective reagent for SH groups, *Biochemistry* 3 (4) (1964) 480–482.
- [41] S. Nury et al., Lipase kinetics at the triacylglycerol–water interface using surface tension measurements, *Chem. Phys. Lipids* 45 (1987) 27–37.
- [42] B. Borgstrom, H.L. Brockman, *Lipases*, Elsevier, Amsterdam, 1984, p. 527.
- [43] S. Rajendran, S.K. Rao, V. Prakash, Effect of pH in the acidic region on the structural integrity of lipase from wheat germ, *Ind. J. Biochem. Biophys.* 27 (5) (1990) 300–310.
- [44] K.S. Rao et al., Structural stability of lipase from wheat germ in alkaline pH, *J. Protein Chem.* 10 (3) (1991) 291–299.
- [45] G. Benzonana, S. Esposito, On the positional and chain specificities of *Candida cylindracea* lipase, *Biochim. Biophys. Acta* 231 (1971) 15–22.

- [46] Sigma, Catalog-Biochemicals, Organic Compounds, and Diagnostic Reagents, 1996.
- [47] M.D. Virtó et al., Kinetic properties of soluble and immobilized *Candida rugosa* lipase, *Appl. Biochem. Biotechnol.* 50 (1995) 127–136.
- [48] H.W. Blanch, D.S. Clark, *Biochemical Engineering*, Marcel Dekker, 1996.
- [49] H. Klump et al., Glutamate dehydrogenase from the hyperthermophile *Pyrococcus furiosus*. Thermal denaturation and activation, *J. Biol. Chem.* 267 (31) (1992) 22681–22685.
- [50] K.S. Yip et al., The structure of *Pyrococcus furiosus* glutamate dehydrogenase reveals a key role for ion-pair networks in maintaining enzyme stability at extreme temperatures, *Structure* 3 (11) (1995) 1147–1158.
- [51] K.B. Song, S. Damodaran, Influence of electrostatic forces on the adsorption of succinylated β -lactoglobulin at the air–water interface, *Langmuir* 7 (1991) 2737–2742.
- [52] M.G. Ivanova et al., Proteins at the air/water interface and their inhibitory effects on enzyme lipolysis, *Colloids Surf.* 54 (1991) 279–296.
- [53] E. Tornberg, The application of the drop volume technique to measurements of the adsorption of proteins at interfaces, *J. Colloid Interface Sci.* 64 (3) (1978) 391–402.
- [54] A.F.H. Ward, L. Tordai, Time-dependence of boundary tensions of solutions. I. The role of diffusion in time-effects, *J. Chem. Phys.* 14 (7) (1946) 453–461.
- [55] K.L. Sutherland, The kinetics of adsorption at liquid surfaces, *Aust. J. Sci. Res. A5* (4) (1952) 683–696.
- [56] M. van den Tempel, E.H. Lucassen-Reynders, Relaxation processes at fluid interfaces, *Adv. Colloid Interface Sci.* 18 (3–4) (1983) 281–301.
- [57] K. Guruprasad, B.V.B. Reddy, M.W. Pandit, Correlation between stability of a protein and its dipeptide composition — a novel approach for predicting *in vivo* stability of a protein from its primary sequence, *Protein Eng.* 4 (2) (1990) 155–161.
- [58] A. Kato, S. Nakai, Hydrophobicity determined by a fluorescent probe method and its correlation with surface properties of proteins, *Biochim. Biophys. Acta* 624 (1980) 13–20.
- [59] K.N. Pearce, J.E. Kinsella, Emulsifying properties of proteins: evaluation of a turbidimetric technique, *J. Agric. Food Chem.* 26 (1978) 716–723.